5. *On the Distribution of Volcanic Ejecta.* (*Part 1.*) *The Distributions of Volcanic Bombs ejected by the Recent Explosions of Asama.*

By Takeshi MINAKAMI,

Earthquake Research Institute.

(Read Nov. 20, 1941.—Received Dec. 20, 1941.)

1. Introduction.

The initial velocity of volcanic bombs and volcanic detritus ejected in the eruptions of volcanoes an important datum in estimating the magnitude of the explosions, the problem has received the attention of a number of investigators,[1] of whom, T. Matuzawa, studied for the first time, quantitatively, the air resistance of bombs in their flight through the atmosphere.

On the other hand, F. v. Wolff studied the problem thermodynamically and obtaind the pressure at the instant of explosions of Santorin, Mont Pelée and Lassen Peak.

The writer investigated the distribution of volcanic bombs in about thirty strong Asama explosions that occurred during April, 1935, and August, 1941, in doing which he studied, besides, the form of the bomb-fall area, the initial velocities of bombs at the time of ejection in these explosions, and the effect of wind on bomb flight.

Generally speaking, volcanoes of andesitic lava differ in the manner of their eruption from basaltic volcanoes. Asama is the most typical andesitic (acidic) volcano and Aso, Ôshima, and Miyake the typical basaltic, (basic) volcanoes. One of the most important features by which the character of eruptions is determined is the viscosity of the lava.

The outstanding characteristic of Asama's explosions is strong detonation and ejection of much juvenile lava, usually ending in a few minutes and returning to the normal state. Another distinguishing property of this volcano is that, even in very active periods, two or more

1) F. OMORI, *Bull. Earthq. Invest. Commit.*, 7 (1914), 11; T. NOMITU and M. NAMBA, *Mem. Coll. Sci., Kyoto. Imp. Univ.*, 15 (1932), 215; T. FUKUTOMI, *Disin*, 1 (1929), 852; T. MATUZAWA, *Bull. Earthq. Res. Inst.*, 11 (1933), 329 and 347; T. NAGATA, *Bull. Earthq. Res. Inst.*, 16 (1938), 714; F. v. WOLFF, *Journ. Geol.* (1938), 521; T. MINAKAMI, *Bull. Volcanol. Soc. Japan.* (1939), 141.

strong explosions on the same day are very rare, usually, several days intervening until the next explosion.

In contrast to this explosion, Mihara,[2] Aso,[3] Miyake,[4] and other basaltic volcanoes are usually much less violent, the amount of ejecta in an explosion being also much smaller, although the number of explosions is much larger, continuing without interuption for several hours for a number of days.

In violent explosions of Asama, a large quantity of ejecta, such as lava blocks and volcanic bombs, with steam and gas, are thrown out at a great velocity from the crater followed immediately by ejections of smaller fragments only, such as ash, with gas and steam, with less velocity for several minutes. Fig. 20 is a photograph that was taken when bombs fell on the mountain side, 20 seconds after the occurrence of the explosion on March 7, 1936.

2. Flight of Volcanic Bombs.

As one method of measuring the intensity of the recent explosions of Asama, the writer studied the velocity of various bombs at the instant of ejection. Usually, the flight of these volcanic bombs is determined by various conditions, namely, the angle at the moment of ejection (angle of emission), the time consumed in the flight, and the angle at which the bomb fell, and other conditions. The initial velocities of various bombs were obtained for thirty explosions during the recent volcanic activity.

For convenience of computing the flight, bombs as nearly spherical as possible were selected, and the mean density of air and the mean velocity of the wind were taken. Further, it is assumed that the vertical component of air resistance affects only the vertical component of flight and the horizontal resistance of air affects only the horizontal component of the motion.

Since, in the present computation, bombs larger than 50 cm in diameter, being mostly dealt with, and the effect of air resistance to bombs of large size, the simplifications and assumptions mentioned above do not seriously affect the result.

---

2) F. OMORI, *Bull. Imp. Earthq. Invest. Commit.*, **79** (1914) II; **8** (1915); N. YAMAZAKI, *Rep. Imp. Earthq· Inv. Commit.*, **73** (1909); S. NAKAMURA, *Rep. Imp. Earthq. Inv. Commt.*, **73** (1909); T. YAGI, *Volcano Asama.*, (1936); T. MINAKAMI, *Bull. Earthq.·Res. Inst.*, **16** (1935), 629, 790.

3) T. NAGATA, *Bull, Earthq. Res. Inst.*, **16** (1938), 714.

4) K. SASSA, *Mem. Coll. Sci., Kyoto Imp. Univ.*, (A) (1935), 255; **19** (1936), 11.

5) H. TSUYA and others, *Bull. Earthq. Res. Inst.*, **19** (1941). 260.

As to the co-ordinates, the origin is taken at the point of outburst in the pit, the x axis in the direction of the horizontal component of the initial velocity of the bomb, y in direction at right angles to the x axis in the horizontal plane, and the z axis upward.

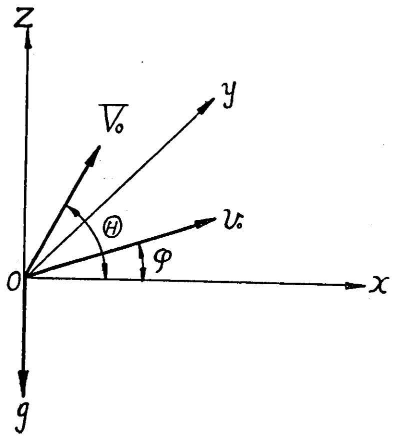

Fig. 1.

As the velocities of the bombs throughout their flight are less than the velocity of sound, it is naturally assumed that resistance of the air is proportional to the square of the relative velocity. Moreover, the direction of the wind blowing in a horizontal plane has an angle of φ to the x axis.

$$m\ddot{x}+c\ (\dot{x}-v_0\cos\varphi)^2=0\,,$$

$$m\ddot{y}+c\ (\dot{y}-v_0\sin\varphi)^2=0\,,$$

$$m\ddot{z}+\delta c\dot{z}^2+mg=0\,,$$

$$\delta=+1 \text{ within the range of } \dot{z}>0,$$

$$\delta=-1 \qquad '' \qquad \dot{z}>0.$$

The initial condition is

$$t=0 \qquad x=y=0,$$

$$\dot{x}=V_0\cos\Theta,$$

$$\dot{y}=0,$$

$$\dot{z}=V_0\sin\Theta.$$

At the point of maximum height attained by the bomb in its flight, the following conditions have to be satisfied:

$$\dot{z}=0,$$

$$z_{\downarrow}=z_{\uparrow},$$

where

$z_{\uparrow}$: motion of elevation,

$z_{\downarrow}$: motion of fall,

$$m=\frac{1}{6}\pi\rho d^3=\text{mass of bomb},$$

$c=\frac{1}{8}k\rho'\pi d^2=$air resistance met by bomb,

$d=$diameter of bomb,

$\rho=$density of bomb,

$\rho'=$mean density of air,

$k=$coefficient of resistance,

$V_0=$initial velocity of bomb,

$\Theta=$angle of ejection,

$v_0=$mean velocity of wind,

and putting

$$\frac{c}{m}=\frac{3k\rho'}{4\pi d}=\lambda,$$

we get

$$x=v_0t\cos\varphi+\frac{1}{\lambda}\log\left\{\lambda t(V_0\cos\Theta-v_0\cos\varphi)+1\right\},$$

$$y=v_0t\sin\varphi-\frac{1}{\lambda}\log(\lambda v_0t\sin\varphi+1),$$

$$z_{\uparrow}=\frac{1}{\lambda}\log\sin\left(\sqrt{\lambda g}\,t+\cot^{-1}\sqrt{\frac{\lambda}{g}}V_0\sin\Theta\right)+\frac{1}{\lambda}\log\sqrt{1+\frac{\lambda}{g}V_0^2\sin\Theta},\quad(\dot{z}\geqq0)$$

$$z_{\downarrow}=-\frac{1}{\lambda}\log\cosh\left(\sqrt{\lambda g}\,t+\tan^{-1}\sqrt{\frac{\lambda}{g}}V_0\sin\Theta\right)+\frac{1}{\lambda}\log\sqrt{\frac{\lambda}{g}}V_0\sin\Theta.\quad(\dot{z}\leqq0)$$

The velocity of the bomb is given by

$$\dot{x}=v_0\cos\varphi+\frac{V_0\cos\Theta-v_0\cos\varphi}{\lambda t(V_0\cos\Theta-v_0\cos\varphi)+1},$$

$$\dot{y}=v_0\sin\varphi-\frac{v_0}{\lambda v_0t\sin\varphi+1},$$

$$\dot{z}_{\uparrow}=\sqrt{\frac{g}{\lambda}}\cot\left(\sqrt{\lambda g}\,t+\cot^{-1}\sqrt{\frac{\lambda}{g}}V_0\sin\Theta\right),$$

$$\dot{z}_{\downarrow}=-\sqrt{\frac{g}{\lambda}}\tanh\left(\sqrt{\lambda g}\,t-\tan^{-1}\sqrt{\frac{\lambda}{g}}V_0\sin\Theta\right),$$

3. Result of computation.

For convenience in determining the velocity of the bomb at the time of explosion, the flights of these bombs under various conditions were studied. An outline of the principal results of the calculation follows.

Figs. 2~4. Horizontal distance (x), horizontal velocity ($\dot{x}$) and time (t). I, I′; $\Theta=30°$, II, II′; $\Theta=35°$, III, III′; $\Theta=40°$, IV, IV′; $\Theta=45°$, V, V′; $\Theta=50°$, VI, VI′; $\Theta=55°$, Θ=angle of emission, V_0=initial velocity of bomb, d=diameter of bomb, v_0=wind velocity.

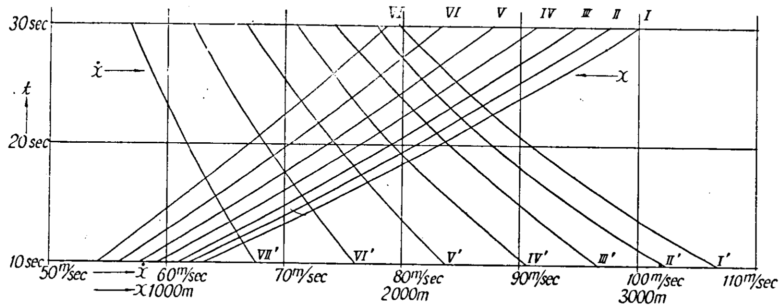

Fig. 2. $V_0=150$ m/sec, $d=50$ cm, $v_0=10$ m/sec.

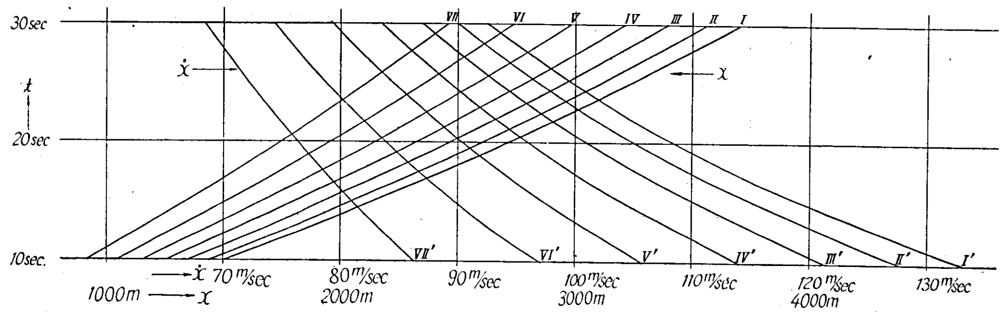

Fig. 3. $V_0=180$ m/sec, $d=50$ cm, $v_0=10$ m/sec.

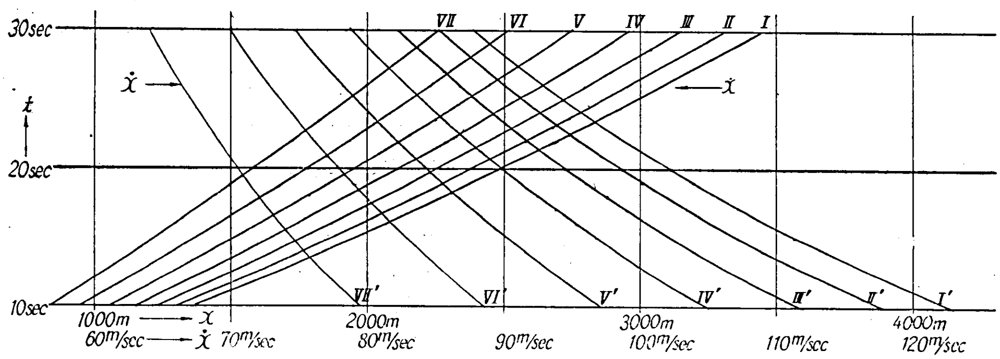

Fig. 4. $V_0=200$ m/sec, $d=50$ cm, $v_0=10$ m/sec.

In Figs. 2∼4 and Table I are given the relation between the time taken in flight and the horizontal distances travelled, and the horizontal velocities of bombs that fall on a slope of 10° of the mountain.

Table I. Flight of bomb.

Θ		H	t_H	t	x	z
		m	sec	sec	m	m
d=50 cm, V_0=150 m/sec	30°	270	7·2	20·2	2180	−530
	35°	340	8·2	22·0	2230	−550
	40°	430	9·1	23·7	2270	−560
	45°	510	9·9	24·9	2200	−540
d=50 cm, V_0=180 m/sec	30°	373	8·6	23·8	2880	−700
	35°	483	9·7	25·9	2940	−720
	40°	591	10·7	27·8	2950	−730
	45°	695	11·5	29·0	2880	−710
	50°	806	12·4	30·6	2800	−690
	55°	902	13·0	31·5	2630	−650
	60°	990	13·6	32·5	2430	−600
d=50 cm, V_0=200 m/sec	30°	456	9·4	26·0	3330	−820
	35°	590	10·6	28·5	3450	−870
	40°	717	11·7	30·5	3450	−870
	45°	842	12·6	31·9	3350	−830
	50°	956	14·1	34·1	3280	−810
	55°	1073	14·8	35·2	3070	−760
	60°	1174	15·4	36·1	2810	−700

Θ=angle of emission,
H=maximum height arrived by bomb,
t_H=time taken to reach maximum height,
t=total time of flight,
x=horizontal distance of place of fall from the crater,
z=vertical distance of place of fall from the crater,
d=diameter of bomb,
V_0=initial velocity of bomb,
ξ=inclination of mountain slope (10°)

In Fig. 5, the vertical velocity and the vertical distance from the crater of bombs that are ejected at various angles of emission, are calculated.

In Fig. 6 are shown the maximum heights, and the horizontal distances from the origin to maximum height, and the time taken for the bombs to reach maximum height, for bombs ejected in various directions.

After the bombs with various diameters arrive at the maximum height, their fall-velocities ($\dot{z}<0$) and the vertical distances of fall ($z<0$) from the maximum height are calculated in Fig. 7 b.

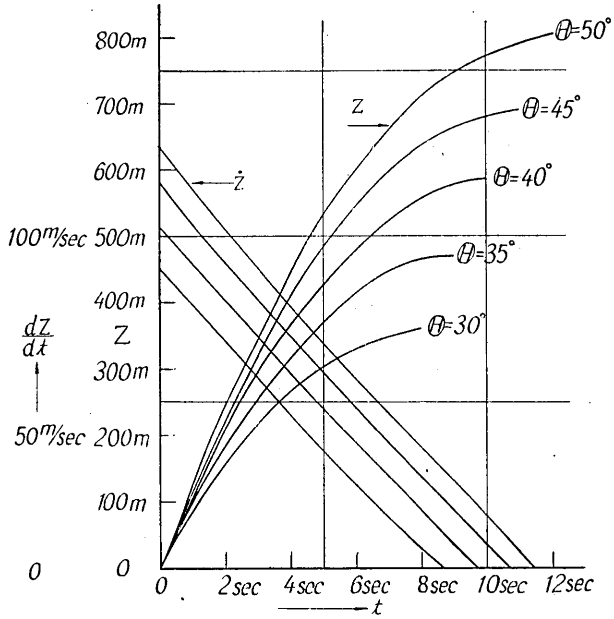

Fig. 5. Vertical distance, vertical velocity and time. $d=50$ cm, $V_0=180$ m/sec.

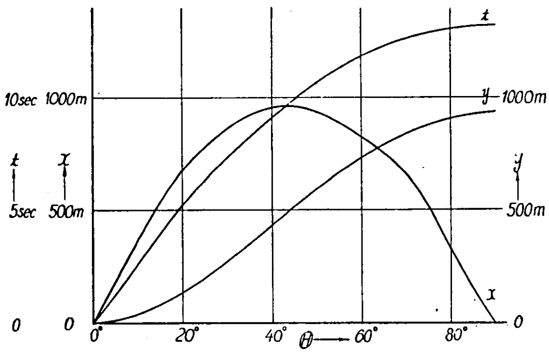

Fig. 6 a. Maximum height (y) time (t) taken from the origin to maximum height, the horizontal distance (x), from the origin and angle of emission. $V_0=150$ m/sec, $d=50$ cm.

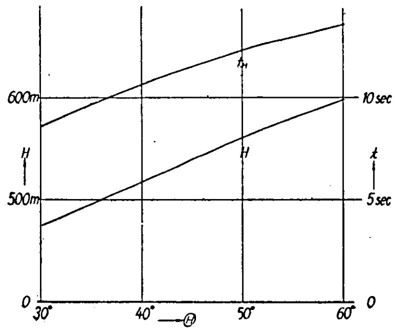

Fig. 6 b. Maximum height (H) and time taken to maximum height from the origin. $V_0=180$ m/sec, $d=50$ cm.

Obviously, air and wind resistance depend on the diameter of the bomb. In order to show the difference in these effects as the result of daimeter, the horizontal distance of travel of the bomb and its velocity were calculated for bombs of diameters of 50 cm, 75 cm, and 100 cm, with results as shown in Fig. 8 and Table II.

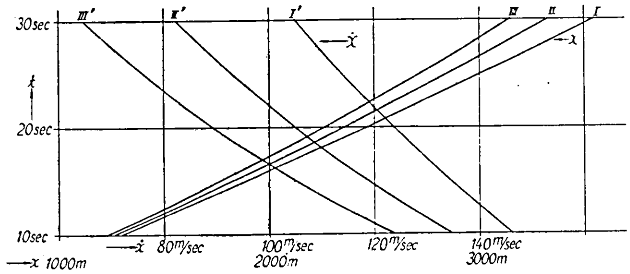

Fig. 7 a. Horizontal distance (x), horizontal velocity ($\dot{x}$) and diameter of bomb (d).
I; d=50 cm, II; d=75 cm, III; d=100 cm.
Θ=40°, v_0=10 m/sec. (wind velocity)

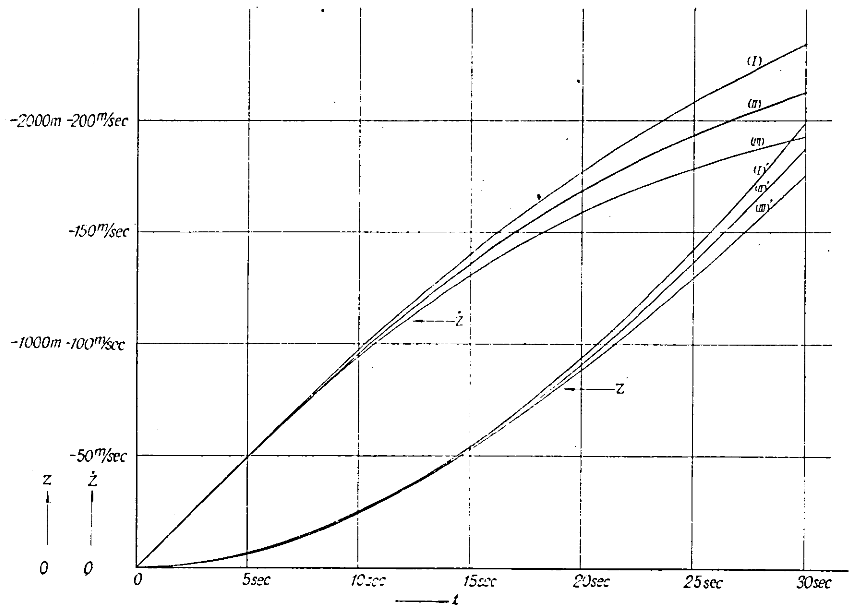

Fig. 7 b. Vertical fall distance (z), vertical fall velocity ($\dot{z}$) and time taken from the maximum height (t).
I; d=100 cm, II; d=75 cm, III; d=50 cm.

The time taken in flight by the bomb from the moment of ejection to its fall on the mountain slope, and the horizontal distances to which they travel from the origin when ejected at various angles of emission were calculated, the results being shown in Fig. 9.

Table II. Initial velocity and diameter and horizontal distance of arrival of bomb.

A				B			
V_0	$x_d=50$ cm	$x_d=75$ cm	$x_d=100$ cm	V_0	$x_d=50$ cm	$x_d=75$ cm	$x_d=100$ cm
m/sec	m	m	m	m/sec	m	m	m
150	2270	2 .50	2580	150	2150	2330	2480
160	2500	2680	2880	160	2350	2570	2750
170	2730	2930	3180	170	2580	2800	3050
180	2950	3160	3480	180	2800	3050	3420
190	3200	3470	3770	190	3030	3310	3650
200	3450	3800	4120	200	3260	3630	3960
210	3750	4130	4480	210	3500	3950	4320
220	4030	4430	5050	220	3780	4250	4870

A { $\Theta=40°$ = angle of emission, $v_0=10$ m/sec = velocity of wind, $\xi=10°$ = inclination of mountain slope.

B { $\Theta=40°$ = angle of emission, $v_0=0$ (no wind), $\xi=10°$ = inclination of mountain slope.

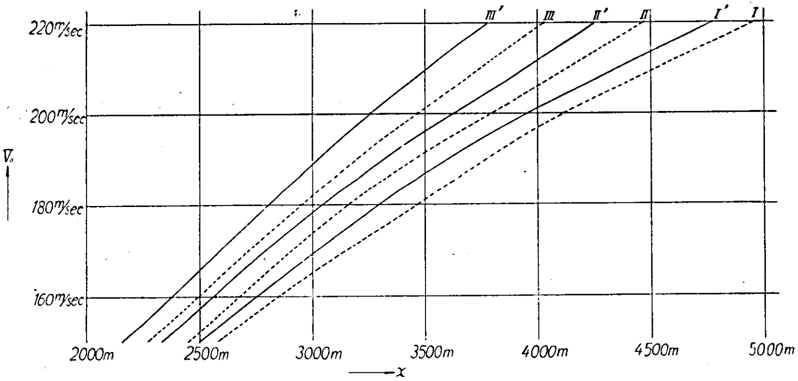

Fig. 8. Initial velocity and horizontal distance of fall.
I; $d=100$ cm, II; $d=75$ cm, III; $d=50$ cm.
$\xi=10°$ = inclination of mountain slope,
$\Theta=40°$,
full line = no wind,
broken line = wind velocity, $(v_0)=10$ m/sec.

Table III. Angle of fall on the mountain slope.

Θ	φ_{I}	φ_{II}	φ_{III}	Θ	φ_{I}	φ_{II}	φ_{III}
30°	52·°3	54·°1	55·°6	50°	62·°6	63·°8	64·°7
35°	55·°5	56·°8	58·°2	55°	65·°0	65·°6	66·°5
40°	57·°7	59·°4	60·°3	60°	67·°3	67·°9	68·°4
45°	60·°3	61·°3	62·°5				

Θ; angle of emission,
φ; angle of fall on the mountain slope,
I, II, III; initial velocity 150 m/sec, 180 m/sec, 200 m/sec, inclination of mountain slope 10°

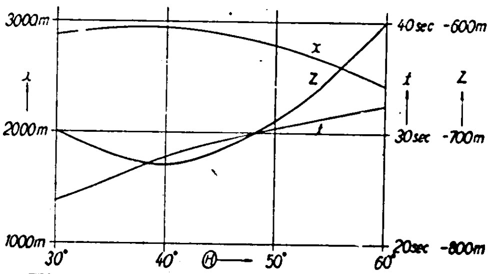

Fig. 9. Total time in flight and arrival distance of bomb.
$d=50$ cm, $V_0=180$ m/sec, $\xi=10°$.

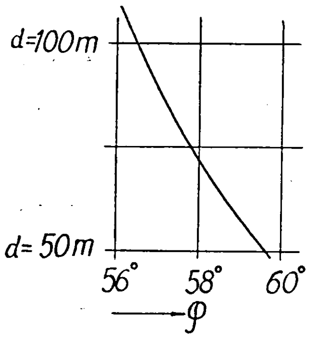

Fig. 11. Angle of fall and diameter of bomb. $V_0=180$ m/sec, $\xi=10°$.

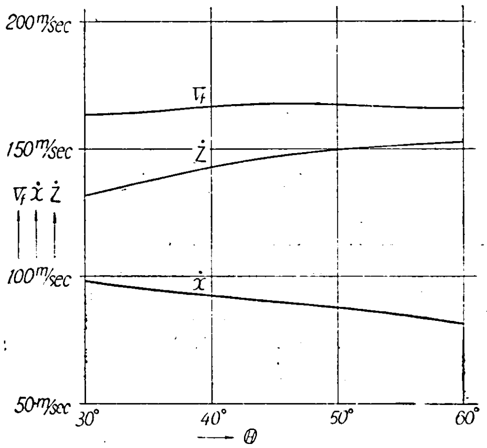

Fig. 12. Fall velocity and angle of emission.
$V_f=(\dot{x}^2\times\dot{z}^2)^{1/2}$, $V_0=180$ m/sec,
$d=50$ cm, $\xi=10°$.

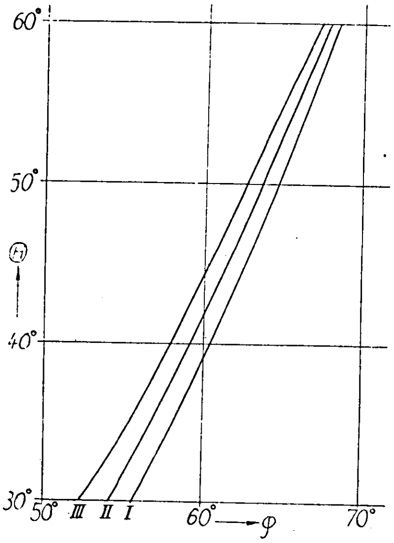

Fig. 10. Angle of emission (Θ) and angle of fall (φ).
$d=50$ cm,
I; $V_0=150$ m/sec,
II; $V_0=180$ m/sec,
III; $V_0=200$ m/sec.

Table IV. Relation between angle of fall and diameter of bomb.

d	φ	d	φ
cm		cm	
100	56·°5	60	58·°8
90	56·°9	50	59·°6
80	57·°5	40	60·°5
70	58·°1		

angle of emission (Θ) $=40°$,
initial velocity $=180$ m/sec,
slope of mountain $=10°$.

The relations between the angles of emission and the angles of fall were calculated for bombs falling with various angles of emission on the surface of the mountain, with results as shown in Table III and Fig. 10, from which it will be seen that the angles of fall are markedly larger than those of emission. This may be explained by the fact that air resistance comes into play, and that the place where the bombs fell is lower than the crater floor.

Table V. Flight of bomb.

Θ		$\dot{x}$	$\dot{z}$	V_f	φ
		m/sec	m/sec	m/sec	
d=50 cm, V_0=150 m/sec	30°	90·6	117·0	148·0	52° 16′
	35°	85·6	123·0	149·8	55 30
	40°	80·3	127·0	150·2	57 45
	45°	75·0	131·0	151·0	60 20
d=50 cm, V_0=180 m/sec	30°	96·0	132·0	163·3	53 59
	35°	90·0	138·0	164·6	56 53
	40°	84·8	144·0	167·2	59 35
	45°	79·8	147·0	167·8	61 19
	50°	74·2	150·0	167·9	63 42
	55°	69·0	152·0	166·9	65 37
	60°	62·6	154·0	166·4	67 54
d=50 cm, V_0=200 m/sec	30°	96·5	141·0	170·8	55 37
	35°	92·0	148·0	174·2	58 12
	40°	86·4	153·0	175·6	60 27
	45°	81·6	156·0	175·9	62 26
	50°	75·6	160·0	176·9	64 43
	55°	70·4	162·0	176·6	66 32
	60°	64·4	163·0	175·2	68 26

$\dot{x}$=horizontal component of velocity at time of fall,
$\dot{z}$=vertical component of velocity at time of fall,
V_f=velocity of bomb at time of fall,
φ=angle of fall,
Θ=angle of emission,
ξ=inclination of mountain slope=10°.

Naturally the angle of fall depends also on the diameter of the bomb. The angle of fall for bombs of various diameters in the case of an initial velocity of 180 m/sec, angle of emission 40°, and 10° inclination of the mountain surface, are given in Fig. 11 and Table IV.

In addition, the velocities at the time of fall on the mountain were computed for various angles of emission, with results as shown in Fig. 12 and Table V.

4. The Explosion of April 16, 1937.

The explosion of April 16, 1937, was one of the most remarkable in the recent activities during 1935 and 1941.

Topographical surveys of the interior of the crater were made on April 13, three days before the explosion, and on April 17, the day following the explosion. As the results of these topographical surveys, changes in the crater floor, both in form and depth, were made clear. The horizontal and vertical distances measured between the point of the explosion in the pit and the edge of the crater-wall are shown in Table VI. After this explosion, the exact positions where the bombs fell and the diameters of these bombs were investigated and the bomb-

Table VI. Result of topographical survey of the crater and the places of fall of bombs. (see Fig. 14.)

(The explosion of April 16, 1937.)

No. 1	r	h	x	z	ξ
	m	m	m	m	
1	258	222	3278	−710	12° 12′
2	235	222	2572	−490	10 46
3	200	222	2719	−450	10 29
4	175	222	2322	−460	11 13
5	145	222	1572	−250	9 3
6	125	222	1646	−300	10 19
7	85	221	1337	−270	11 22
8	82	220	1205	−160	7 32
9	75	221	1117	− 90	4 35
10	70	222	1014	−230	12 44
11	60	224	867	+ 50	− 3 10
12	58	226	793	+ 90	− 6 30
13	50	228	779	+ 90	− 6 34
14	55	230	911	− 10	6 17
15	70	228	1073	−160	8 29
16	85	226	1131	−170	8 32
17	105	224	1440	−350	13 40
18	115	222			
19	145	225	1999	−550	15 23
20	170	217	2707	−620	15 0
21	205	215	2940	−710	13 33
22	250	212	2483	−910	15 58
23	270	213	3454	−850	13 49
24	275	214	3175	−780	13 46

fall area obtained. The result is given in Fig. 13 with a rough topographical map of the volcano. It should be noted that the bombs shown in the distribution map are only those that fell farthest away from the crater, in all directions, those that fell near the crater being excluded.

In order to give in outline the changes in the crater-floor caused by the explosion, an E-W profile of the crater is shown in Fig. 14, from which it will be seen that the surface of the pit before the explosion was quite flat, whereas by the explosion, the western part of the pit, with a volume of about 50 m × 50 m × 30 m, was thrown out in the form of lava blocks, volcanic sand and ash. Although most of this material fell outside the crater, a part of it had either fallen back into the crater or was prevented by the crater-wall from leaving the crater, with the result that they accumulated on the eastern floor of the crater.

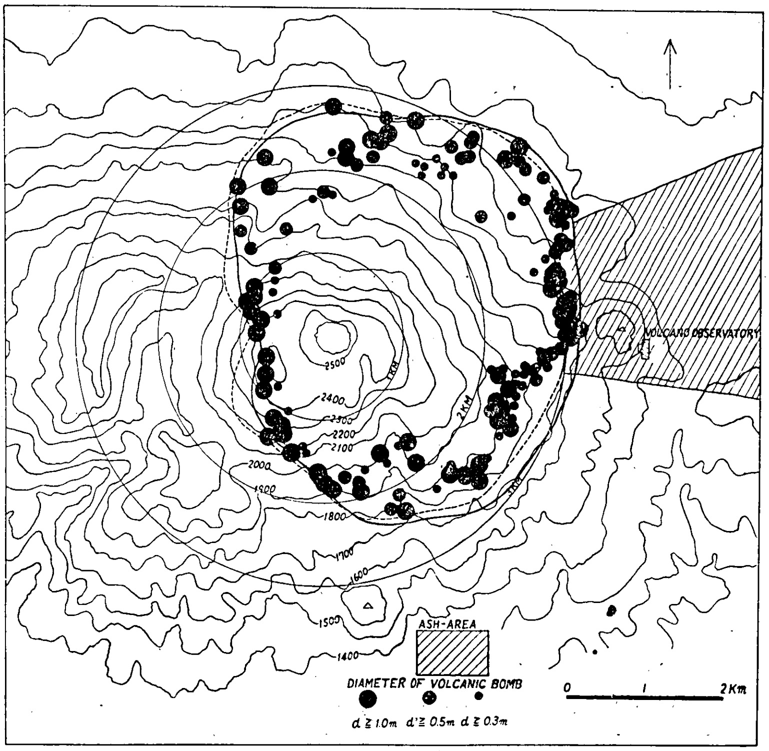

Fig. 13. Distribution of volcanic bombs in the explosion of April 16, 1937.
broken closed curve (I)
full closed curve (II)

At the same time, in the north-eastern part of the volcano, near the Temmei lava flow "Oni-osi-dasi," a number of bombs fell in the woods and injured the trees. For this reason, the angle of fall of these bombs were obtained by measuring the scars on the trees and the positions of these bombs on the ground.

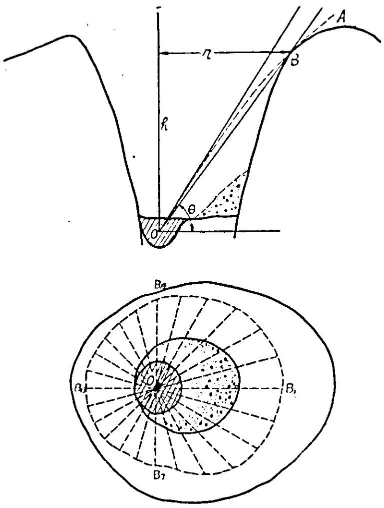

Fig. 14. E-W profile and plan of the crater.

Table VII.

No.	d	φ	x	z
	cm		m	m
1	90	60°	3450	−850
2	75	57	3320	−835
3	60	59	3000	−830

where

d = diameter of bomb,

x = horizontal distance between the origin of emission and the place of fall,

z = vertical distance between the origin of emission and the place of fall,

φ = angle of fall.

From these data, the initial velocities and the angles of emission were computed, as follows:

Table VIII.

No.	V_0	Θ	No.	V_0	Θ
	m/sec			m/sec	
1	168	43°	3	166	42°
2	173	37			

where

V_0 = initial velocity,

Θ = angle of emission.

By calculation, the initial velocities of these bombs show almost the same value of nearly 170 m/sec.

The mean initial velocity obtained for these bombs is 167·0 m/sec ± 3·6 m/sec.

On the other hand, as will be seen from Fig. 13, in the distribution of bombs, those on the eastern side travelled a markedly greater distance from the crater than those on the western side, the former distance being almost five times that of the latter. From this fact, and from the manner in which the ejecta had accumulated on the floor of the crater, it may be reasonable to suppose that the range of angle of emission within which it is possible for the bombs to leave the crater, is an important factor in the distribution of the bombs, so that the angle of emission with which the bombs reach the greatest distance from the crater was studied for the case of constant initial velocity and for various diameters of bombs.

Table IX. Angles of emission, diameters of bombs and initial velocities of bombs.

(The explosion of April 16, 1937.)

No.	Θ	α	d	V_0
			cm	m/sec
1	43° 14′	39° 50′	100	172
2	45 48	40 35	78	169
3	50 9	42 15	60	175
4	53 52	41 21	45	169
5	58 43	42 28	50	162
6	62 15	41 48	45	165
7	70 11	41 17	40	168
8	70 45	43 10	48	163
9	72 21	43 42	52	162
10	73 31	39 38	55	161
11	74 46	48 54	35	150
12	76 27	50 30	30	163
13	78 22	49 35	50	160
14	77 20	42 41	80	164
15	73 55	42 12	60	161
16	70 24	42 38	40	153
17	66 15	40 16	30	162
18	64 5			
19	58 56	38 24	47	165
20	53 58	38 27	105	169
21	48 36	39 11	90	172
22	42 48	37 57	100	180
23	41 0	39 2	100	180
24	40 34	39 5	95	179

To illustrate, for the case in which the diameter, initial velocity, and the inclination of the mountain are 50 cm, 180 m/sec, and 10° respectively, bombs with an angle of emission of 39° travel the greatest distance (see Fig. 9). The angle (α) of emission of bombs that travel the farthest were obtained for all directions from the crater, with results as shown in Table IX. Naturally in these calculations, the effect of air and wind resistance at the time of explosion have been allowed for.

At the same time, the minimum angles of emission for all the directions in which it is possible for the bombs to travel from the origin of the explosion to points outside the crater were obtained from topographical surveys of the crater.

That is, the minimum angles of emission defined above were obtained from the formula

$$\Theta=\tan^{-1}\frac{h+\frac{1}{2}\left(\frac{s}{V_0}\right)^2 g}{r},$$

where

$s \doteqdot \sqrt{h^2+r^2}$ = distance travelled by a bomb from the origin of explosion to the edge of the crater (see Fig. 14).

r = horizontal distance between the center of explosion and the edge of the crater-wall,

h = vertical distance between the center of explosion and the edge of the crater-wall,

V_0 = initial velocity of bomb (approximate value = 180 m/sec),

g = gravity acceleration.

The angles of emission for the 24 directions in which the bombs flew, as mentioned above, are shown in Table IX.

These two kinds of emission, defined above, namely Θ and α, were then compared with each other for all the corresponding directions, with the result that the angle α is less than Θ (Fig. 15), that is to say, that on account of the crater-wall, it was impossible for bombs thrown out with angle of emission α in whatever direction to fall outside the crater. Consequently, it is concluded that the angles of emission with which the bombs travelled the farthest are the minimum angles of emission Θ with which it is possible for the bomb to leave the crater.

The minimum angle of the 23 rd direction, obtained from the topographical survey, is 40° 34′, and the angle of emission for the same direction calculated by the angle of fall (see Table VIII) is 41° 0′, the two results agreeing sufficiently well.

By assuming that these bombs reached the most distant places, travelling with the minimum angle of emission for each direction, the initial velocities of these bombs for every direction were obtained. In the present case, of the many bombs that fell in the same direction,

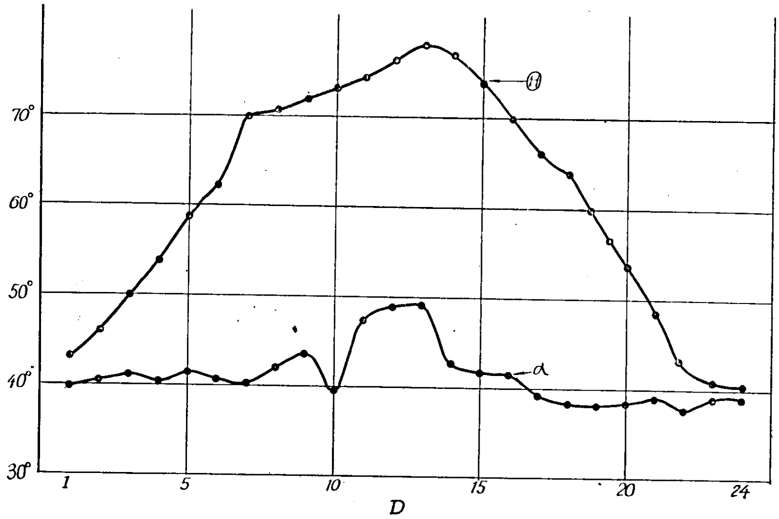

Fig. 15.

θ=minimum angle of emission possible to travel from the crater,
α=angle of emission to arrive at the farthest distance.
D=radial direction from the center of explosion to the foot of the mountain.

the one that gave the largest velocity was selected for our purpose.

The initial velocities of the bombs for twenty-four directions and the calculation are shown in Table VIII, from which it will be seen that the initial velocities of the bombs for all directions are almost 160 m/sec and 170 m/sec, the mean value being 166·3 m/sec.

In contrast to this, when a bomb, 50 cm in diameter, is ejected with an initial velocity of 166·3 m/sec and with the angles of emission (θ) for all the corresponding directions from the crater into which they flew, the distances travelled by the bombs were computed for every direction.

In Fig. 13, the result of calculation is shown by the closed curve I. Besides, the wind, which had a mean velocity of 10 m/sec, and which was blowing in an easterly direction at the time of the explosion, was allowed for in calculating the distances travelled by these bombs. The result is also shown by closed curve II, in the same map. As will be seen from Fig. 13, although these two curves pass through almost the outer margin of the bomb-fall area, closed curve II is closer to the bomb-fall area than is closed curve I.

Summarizing these results, it is concluded that all these bombs from the explosion on April 16, 1937, were ejected with almost the same velocity of 166 m/sec, the bombs that travelled farthest from the crater leaving it with the minimum angle of emission for their respective directions. At the same time, the phenomenon is interpreted from the stand point that the form of the bomb-fall area is a shadow of the edge of the crater-wall.

The volcanic bombs and the holes they made in the ground are shown in the photographs, Figs. 26 and 27.

5. The Explosion of April 20, 1935.

Asama had been quiet for three years since 1932, the explosion on April 20, 1935, being the first of the present activity to break the serenity.

The writer believed that the elevations and subsidences of the crater floor is closely related to volcanic activity, for which reason, since 1934, a number of topographical surveys of the crater had been made, with the result that deformations of the pit caused by the explosion were clearly shown by the surveys made both before and immediately following the explosion.

The result of these surveys[6] were reported in previous papers.

In the present outburst, the center of explosion on the crater-floor, that is, the point in the pit whence the lava was ejected, was nearly its center.

From investigations made of the bomb-fall area (see Fig. 16) the outer edge of the bomb-area was everywhere nearly of the same distance from the crater.

By the method just mentioned, the angles of emission (α) of the bomb, with which it may travel the farthest, free from obstruction by the crater-wall, were obtained for twenty-four directions from the crater.

Since the bombs that fell on the ground near the outside of the bomb-fall area are mostly those of diameters exceeding 70 cm, in the two kinds of angle of emission, air resistance has been allowed for in one and not in the other, the difference between them being comparatively small for bombs of large diameter, such as those exceeding 70 cm. When bombs with diameters of 100 cm and 50 cm, ejected with an initial velocity of 150 m/sec, fall on the mountain side with 10° in angle of slope, the difference ($\Delta\alpha$) in these two kinds of angles of emission are nearly 1° and 3° respectively.

6) T. MINAKAMI, *Bull. Earthq. Res. Inst.*, **13** (1935), 318; **15** (1937), 492.

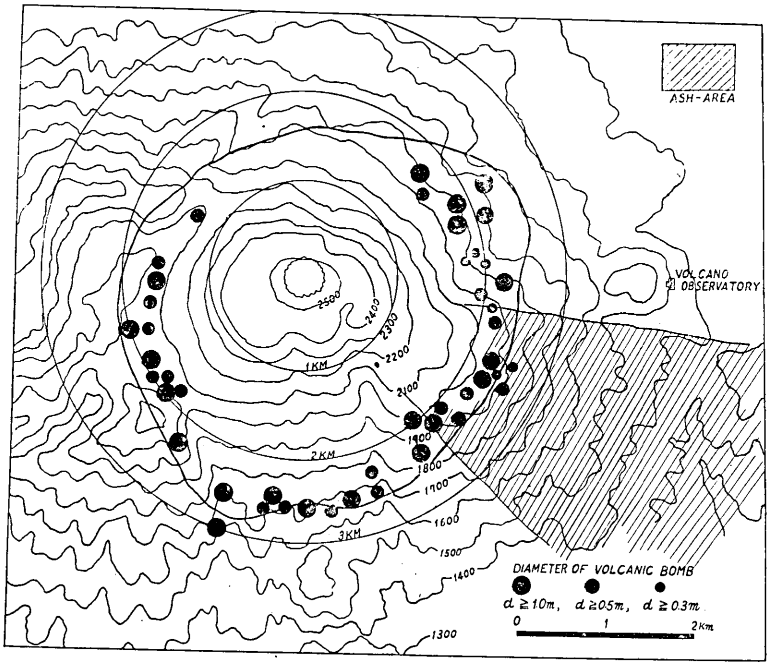

Fig. 16. Distribution of volcanic bombs in the explosion of April 20, 1935.

Table X. Result of topographical survey of the crater and the places of fall of bombs, ejected by the explosion of April 20, 1935.

No.	r	h	x	z	ξ
	m	m	m	m	
1	180	214	2200	−525	13° 23′
2	192	214	2220	−455	11 39
3	205	214	2250	−455	11 26
4	220	214	2250	−505	12 38
5	235	214	2270	−565	13 56
6	240	214	2500	−635	14 15
7	225	214	2750	−705	14 22
8	225	212	2700	−905	18 31
9	200	213	2850	−905	17 39
10	190	214	2000	−355	10 6
11	170	216	1950	−265	7 45
12	150	218	2220	−355	9 12
13	125	220	1750	−255	8 19
14	115	222	1500	−305	11 32
15	100	220	1400	−225	9 9
23	150	199	1700	−505	16 30
24	165	194	2000	−705	18 33

For convenience of calculation, the angle of emission (α) is obtained by the sum of the two values, namely,

$$\alpha=\alpha'+\varDelta\alpha,$$

α' = angle of emission with effect of air resistance neglected,

$\varDelta\alpha$ = correction for air resistance.

The arrival distance of the bomb in which the resistance of air is neglected, and in which gravity alone is allowed for, is given by

$$x=\frac{2V_0^2}{g}\cos\alpha'(\tan\xi\cos\alpha'+\sin\alpha')\ .$$

The angle of emission to enable maximum horizontal travel is obtained from the condition,

$$\frac{dx}{d\alpha'}=0\ ,$$

Table XI. Angles of emission, diameters of bombs, and initial velocities of bombs ejected by the explosion of April 20, 1935.

Direction	Θ	α	d	V_0
			cm	m/sec
1	50° 12′	39° 15′	75	144
2	48 22	40 18	80	140
3	46 37	40 16	100	140
4	44 45	40 7	65	145
5	42 50	38 58	95	140
6	42 22	38 45	105	142
7	44 5	36 40	110	146
8	43 50	37 6	100	145
9	47 22	40 52	100	151
10	48 32	42 5	75	146
11	51 27	41 29	70	143
12	55 36	44 1	100	147
13	60 24	44 21	75	150
14	62 30	42 24	50	153
23	52 17	38 23	50	140
24	49 37	37 21	40	147

whence the angle of emission for the purpose is

$$\alpha' = \sin^{-}\left\{\frac{1}{2} - \tan\xi(1+\tan^2\xi)^{-\frac{1}{2}}\right\}^{\frac{1}{2}},$$

where

x = horizontal distance of fall of bomb from the crater,

ξ = inclination between the horizontal and the line connecting the origin of explosion and the location of fall of bomb,

whence the angle of emission with the resistance of air allowed for is given in the foregoing paragraphs, the results of calculation being shown in Table XI.

Obviously, the correction $\Delta\alpha$ depends not only on the diameter of the bomb, but also on the initial velocity, and the inclination of slope of the mountain.

$\Delta\alpha$	d
	cm cm
1°～2°	100～75
2°～3°	75～40

On the other hand, the minimum angles of emission Θ to enable the bombs to leave the crater are obtained by the method already discribed, and from the topographic surveys made soon after the explosion, the result being shown in Table XI,

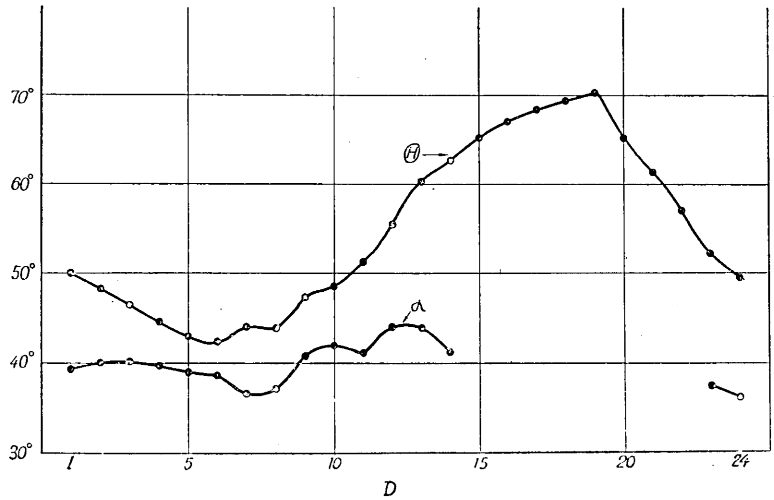

Fig. 17.

Θ and α = angles of emission above defined,
D = direction from the crater to the bomb-fall area.

However, by comparing the two kinds of angles, we find that the following relation obtains for all directions from the origin of explosion (see Fig. 17) namely,

$$\theta > \alpha .$$

That is, the angle θ for all directions exceeds angle α, whence it is known that owing to the crater-wall, the bombs were prevented from leaving the crater with the angle of emission α, and that the bombs that travelled the farthest were those with minimum angle of emission θ.

The initial velocities for these bombs were calculated by the same method as for the explosion of April 16, 1937. As the mean velocity and the direction of the wind at the time of the explosion, 5 m/sec and E 20° S were taken in the calculation.

The result of calculation, and the diameters of the bombs considered for the purpose, are given in Table XI. It was made clear that the initial velocities of the bombs that fell on the edge of the bomb-fall area lie in the range between 151 m/sec and 140 m/sec, and that the mean velocity is 144·5 m/sec.

Moreover, for bombs with initial velocity 144·5 m/sec and a diameter of 100 cm that were ejected with their respective minimum angles of emission for each direction, their destinations are shown by the closed curve in Fig. 16.

From the distribution of the bombs and the calculations just mentioned, almost the same conclusion as that mentioned in the preceeding paragraph is reached concerning the extent of the bomb-fall area, and that the form of this area is a shadow of the edge of the crater-wall, taking the centre of eruption in the crater floor as the source.

6. The Explosion of June 7, 1938.

In the quantity of ejecta, the intensity of detonation, and the severity of earth-shaking, the explosion of June 7, 1938, outclasses the nearly three hundred that occurred during 1935 and 1941.

Besides, in the present explosion, unusually large lava blocks were ejected. One of them, which fell 300 m southeast of the crater, has a diameter of 7·5 m and weighs about $3{\cdot}4 \times 10^5$kg. Figs. 21~23 show these lavablocks photographed from three directions. Bombs almost 100 cm in diameter flew over Ko-Asama, a parasitic cone on the eastern slope of the volcano and at a distance of 3·5 km from the crater, and fell near the Kusatu-Kutukake road, 4·5 km from the crater.

Moreover, a number of volcanic bombs fell on the eastern foot of Ko-Asama. These bombs were very hot, about 800°C at the time they fell, with the result that those which fell in the woods started fires there.

The exact positions where the large bombs fell on the eastern slope of the mountain may be seen from Fig. 18.

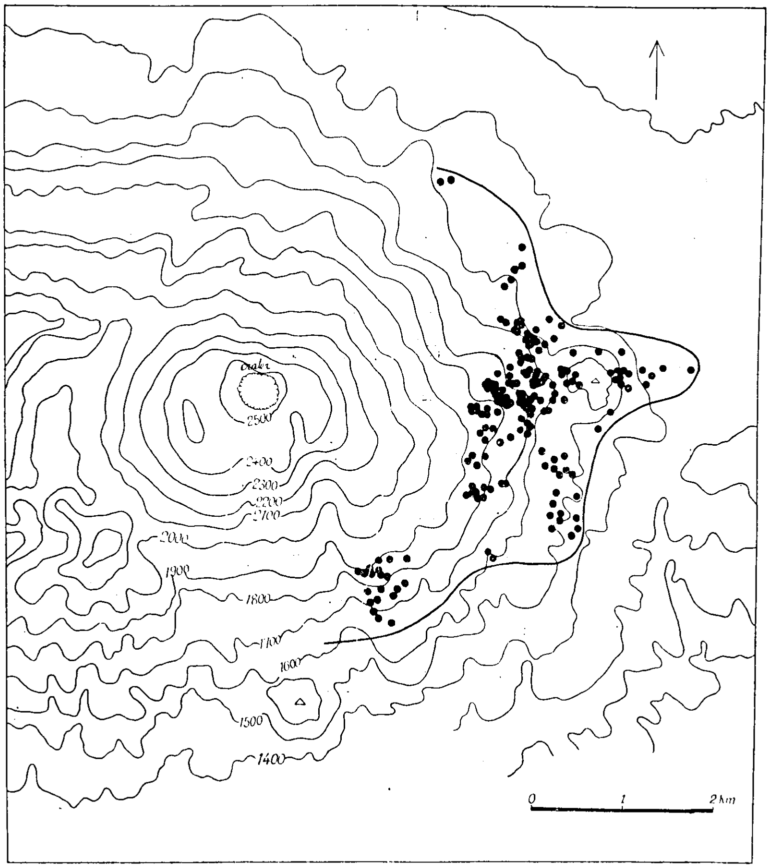

Fig. 18. Distribution of volcanic bombs in the explosion of June 7, 1938.

Since the topographical survey of the crater immediately following the explosion and full investigations of the bomb-fall area were not executed, the exact point of origin of the explosion on the pit is not known. It is not, however, difficult to suppose, from the eastern distribution of bombs, that the form of the bomb-fall area is larger on the eastern side of the volcano than on the western.

The angle of fall of the bombs that fell in the woods at the foot of Ko-Asama, were measured, together with their distances from the crater.

Result of measurement of the angle of fall:

x = horizontal distance from the crater,

z = vertical distance from the bottom of the crater,

φ = angle of fall,

d = diameter of bomb.

Table XII.

x	z	φ	d	x	z	φ	d
m	m		cm	m	m		cm
3700	−900	61° 30′	52	4100	−1000	58° 50′	74
3950	−970	59 50	65				

From these measurements the mean initial velocity of these bombs works out to

$$V_0 = 212{\cdot}5\ \text{m/sec} \pm 5\ \text{m/sec},$$

their angles of emission being within the range

$$\Theta = 40° \pm 3°.$$

In the eastern part of the bomb-fall area, from which the ash-fall area is excluded, the diameters of minimum sized bombs that fell on every space of $100 \times 100\ \text{m}^2$ was measured from the eastern end of the bomb-fall area, that is 4·5 km away from the crater, inward in the bomb-fall area up to a distance of 2 km from the crater, in doing which, bombs that fell broken were excluded. The relation between the minimum sized bombs above mentioned and the distance from the crater, is shown in Fig. 19. The distances travelled by bombs of various diameters from the crater to the surface of the eastern slope of the mountain, with an initial velocity of 212 m/sec and emission angle of 40°, were calculated. As will be seen from the result of calculation shown by curve I in Fig. 19, the curve almost coinsides with the distribution of minimum sized bombs, whence it may be reasonable to conclude that in bombs of various diameter ejected under like conditions, the distances they travel depend on their size, and that it has been shown that the

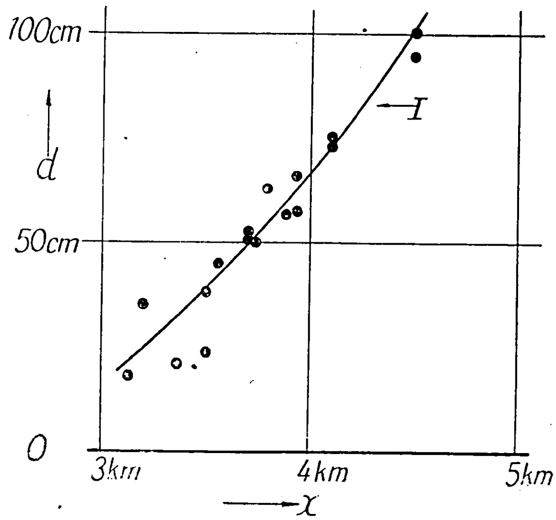

Fig. 19. Diameters of minimum sized volcanic bombs and distance of arrival.

bombs of various diameters ejected by an explosion have nearly the same initial velocity.

7. The Explosion of February 7, 1936.

The explosion of February 7, 1936, was not so violent as the preceding three already described. Explosions of this severity were fairly frequent during 1935 and 1941. Figs. 20 are photographs of the bombs at the instant they fell, namely, twenty seconds and thirty five seconds after the explosion, as seen from our Volcano Observatory.

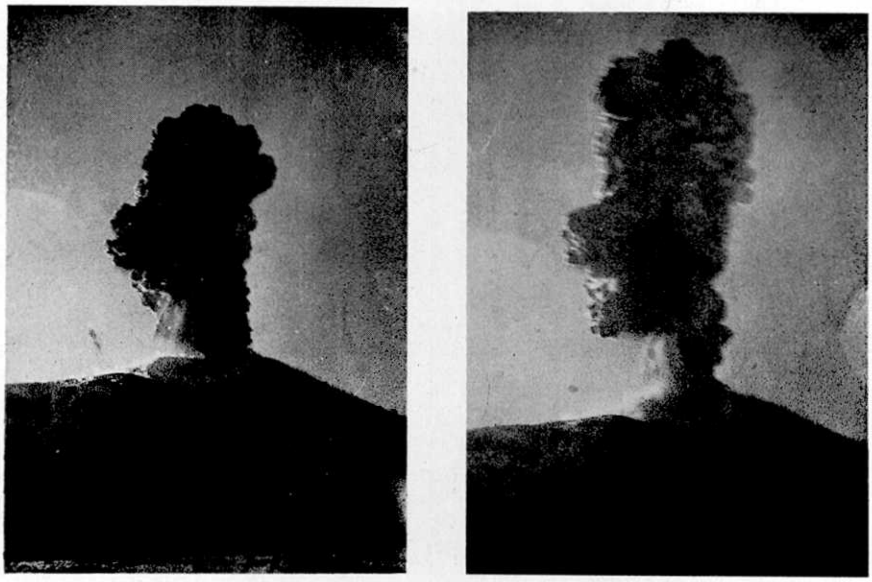

a b

Fig. 20.
a=20 seconds after the explosion,
b=35 seconds after the explosion.

The times taken by the bombs in their flight and the distances travelled by them were measured, and their initial velocities obtained. See example below.

	Diameter of bomb	50 cm	Observation
place of fall	Horizontal distance from the crater	2500 m	Observation
place of fall	Vertical distance from the crater	−500 m	Observation
	Time taken in flight	20 sec	Observation
	Calculated initial velocity of bomb	130 m/sec	

8. Kinetic Energy of the Asama Explosions.

The various results described above may be summarized as follows:

I. From the various elements for determining the flight of bombs, their initial velocities were obtained.

II. These initial velocities of ejection by the same explosion are nearly the same.

III. From topographic surveys made both before and immediately following the explosion, and from investigations of bomb-fall areas, the mass ejected by each explosion was estimated, from which various results were obtained, among which the kinetic energy necessary for imparting the initial velocity to the ejecta was found to be

$$K.E.=\frac{1}{2}MV_0^2,$$

where

M=mass of ejecta,

V_0=mean velocity of ejecta at instant of ejection.

Also, from continuous observations[7] of variations in inclinations of the earths' surface at two or three stations at the foot of the volcano, it was made clear that the unusual variations in the inclination of the ground, which amounted sometimes to thirty or fifty seconds of arc, occurred, preceding the explosion swarms, whence it may be reasonoble to suppose that these unusual tilts of the ground were caused by variations in pressure inside the volcano, that is in the active magma.

Increased pressure causes outbursts of bombs, and reduction of pressure imparts velocity to the bombs and ash.

T. Matuzawa,[8] who is of the opinion that Bernoulli's law practically holds in the pressure and the velocity of ejecta at the instant of explosion, gave the pressure at the time of explosion by the relation,

$$P=\frac{1}{2}\rho V_0^2,$$

where

ρ=mean density of ejecta,

V_0=initial velocity of ejecta.

The following kinetic energy and pressure at the instant of explo-

7) T. MINAKAMI, *Bull. Earthq. Res. Inst.*, **16** (1938), 372.

8) T. MATUZAWA. *loc. cit.*

sion were obtained for these four explosions described above.

I. The explosion of April 20, 1935.

$M=2{\cdot}2\times10^{11}$grm, $V_0=144{\cdot}5$ m/sec, $\rho=2{\cdot}5$,
$K.E.=2{\cdot}3\times10^{19}$erg, $P=260$ atm. pres.

II. The explosion of February 7, 1936.

$M=0{\cdot}81\times10^{11}$grm, $V_0=130$ m/sec, $\rho=2{\cdot}5$,
$K.E.=0{\cdot}68\times10^{19}$erg, $P=210$ atm. pres.

III. The explosion of April 16, 1937.

$M=3{\cdot}0\times10^{11}$grm, $V_0=166{\cdot}3$ m/sec, $\rho=2{\cdot}5$,
$K.E.=4{\cdot}2\times10^{19}$erg, $P=336$ atm. pres.

IV. The explosion of June 7, 1938.

$M=3{\cdot}8\times10^{11}$grm, $V_0=212{\cdot}5$ m/sec, $\rho=2{\cdot}5$,
$K.E,=1{\cdot}7\times10^{20}$erg, $P=563$ atm. pres.

Resumé

In violence, the explosion of June 7, 1938, was the most remarkable within recent years. The total mass of ejecta, the initial velocity of ejecta, the kinetic energy of ejection, and the pressure are $3{\cdot}8\times10^{8}$kg, $212{\cdot}5$ m/sec, $1{\cdot}7\times10^{20}$erg, and 563 atm. pres. respectively. It is supposed that this explosion is the upper limit in magnitude for the Asama volcano, with the exception of catastrophic activity, such as the explosions of the Temmei era.

The magnitude of Asama explosions, as frequently displayed in the recent activities which will probably be repeated a number of times hereafter, is less than 150 m/sec in its initial velocity, lower than 300 atm. pres. in the pressure, and less than 10^{19}ergs in kinetic energy.

In conclusion, the writer wishes to record here his indebtedness to the Hattori Hôkôkai, to the Foundation for the Promotion of Scientific and Industrial Research of Japan, and to the Department of Education, with the aid of whose grants the present study was made possible.

5. 火山噴出物の分布 (其の 1)

最近の淺間火山の爆發により噴出せる火山彈の落下分布

地震研究所 水 上 武

昭和 10 年 4 月より昭和 16 年 12 月に至る約 6 年の間に淺間火山は 300 回以上の爆發が發生した．その中最も顯著な昭和 10 年 4 月 20 日，同 12 年 4 月 16 日，及び同 13 年 6 月 7 日の爆發で噴出した火山彈の落下域を調査した．

又之等の火山彈噴出の際の速度を空氣の抵抗及び風の影響を考慮に入れて計算した．その結果，同じ爆發で噴出した多數の火山彈は略等しい初速度を以つて噴出した事が判つた．又火山彈落下域の形は火口の深さ，及び火口底に於ける爆發發生の位置と火口緣の相對的位置によつて定まる事が判つた．

更に爆發前後に行つた火口內の地形測量の結果及び落下火山彈及び落下火山灰の調査から噴出せる熔岩量を定めた．その結果爆發に働いた Kinetic energy を求めた．又爆發時の壓力と噴出物の速度との間に Bernoulli の法則が成立するものと考へて，その壓力を求めた．

その結果，最近 10 年間に於ける最大の爆發は昭和 13 年 6 月 7 日の爆發であつて

噴出物の初速度	212·5 米/秒
噴出物の質量	$3{\cdot}8\times10^{11}$ 瓦
爆發時の壓力	563 氣壓
爆發のエネルギー	$1{\cdot}7\times10^{20}$ エルグ

と云ふ結果になつた．

比較的頻繁に發生する爆發の壓力，エネルギーは，200 氣壓，$0{\cdot}7\times10^{19}$ エルグ程度のものである．

Figs. 21~23. Lava blocks ejected in the explosion of June 17, 1938.

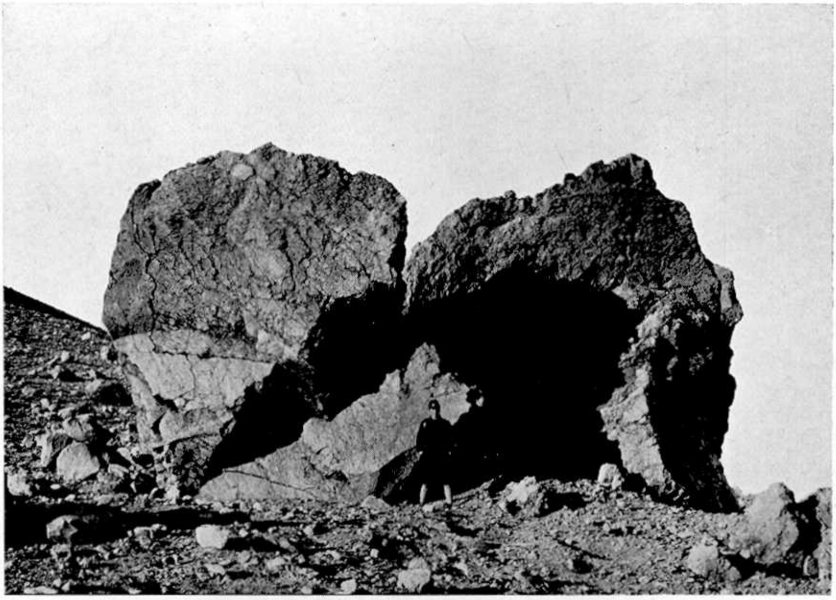

Fig. 21. Seen from the south.

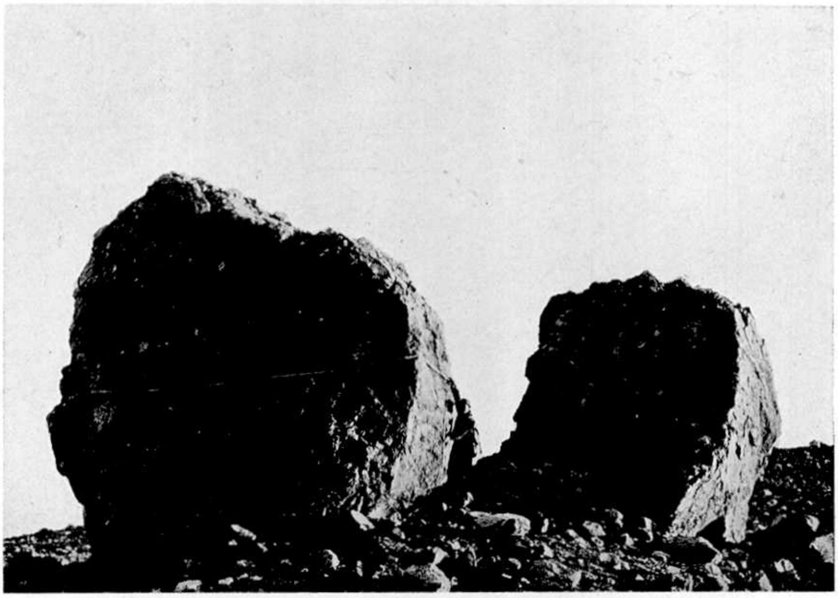

Fig. 22. Seen from the north.

(震研彙報 第二十號 圖版 水上)

(震研彙報 第二十號 圖版 水上)

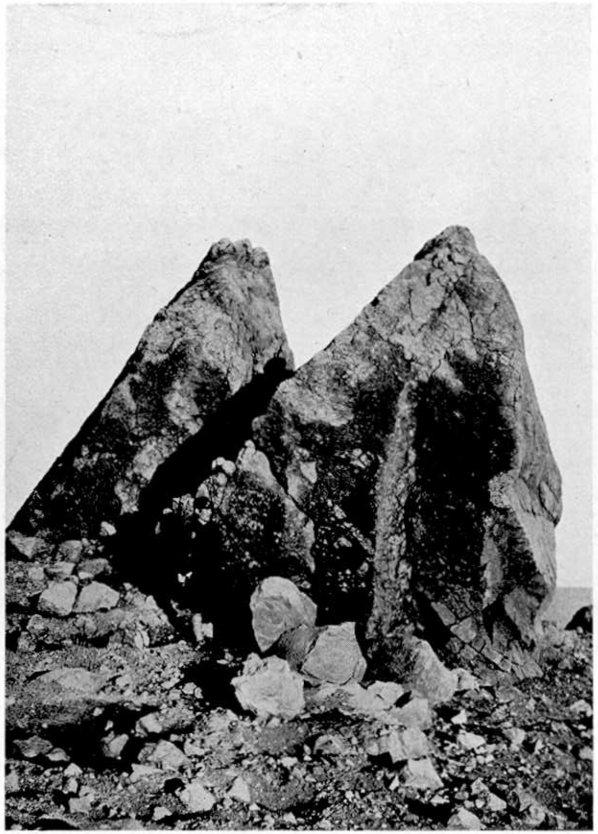

Fig. 23. Seen from the west.

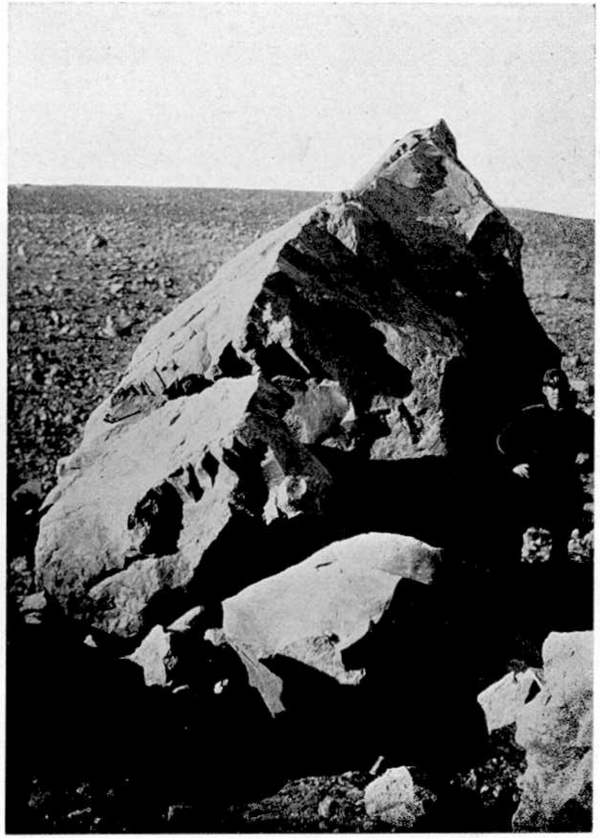

Fig. 24. Large bomb ejected in the explosion of June 7, 1938.

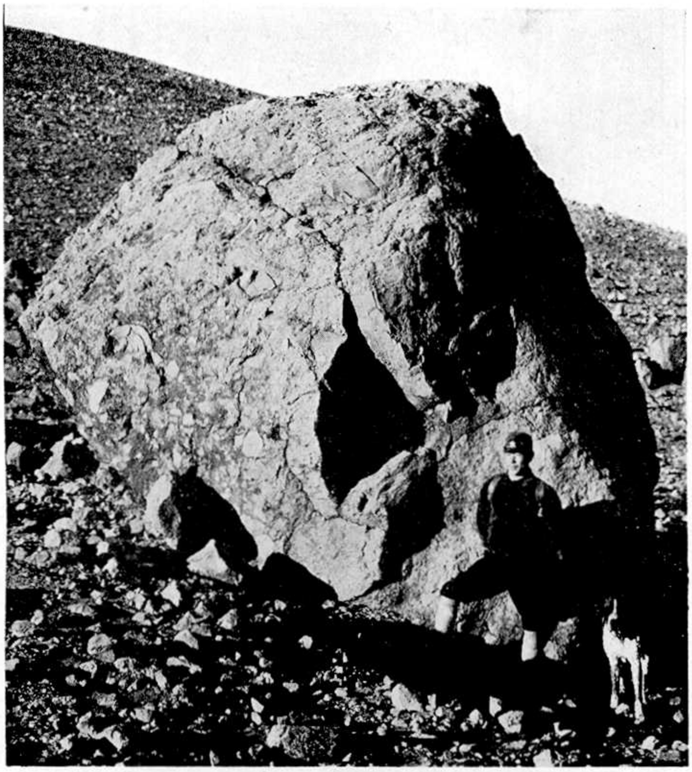

Fig. 25. Large bomb ejected by the explosion of June 7, 1938.

Fig. 26. Large bomb ejected by the explosion of April 16, 1937.

(震研彙報 第二十號 圖版 水上)

Fig. 27. Large hole made on the slope of the mountain by the fall of a bomb in the explosion of April 16, 1937.

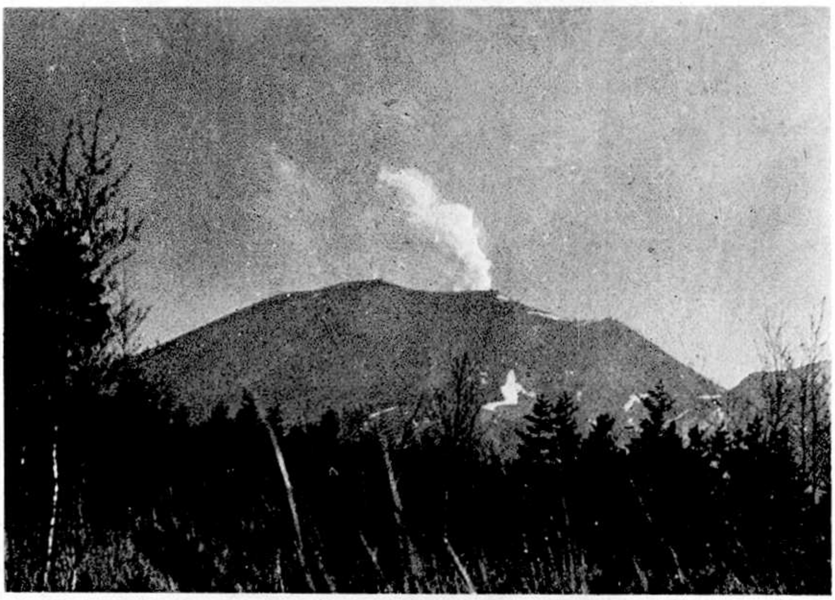

Fig. 28. Asama, the the day after the explosion of April 16, 1937. (seen from the north of the volcano). The gas emits from only the western floor of the crater, where the explosion occurred (see Fig. 14).

Fig. 29. A hole made at the foot of Ko-Asama by the fall of a bomb in the explosion of April 16, 1937.

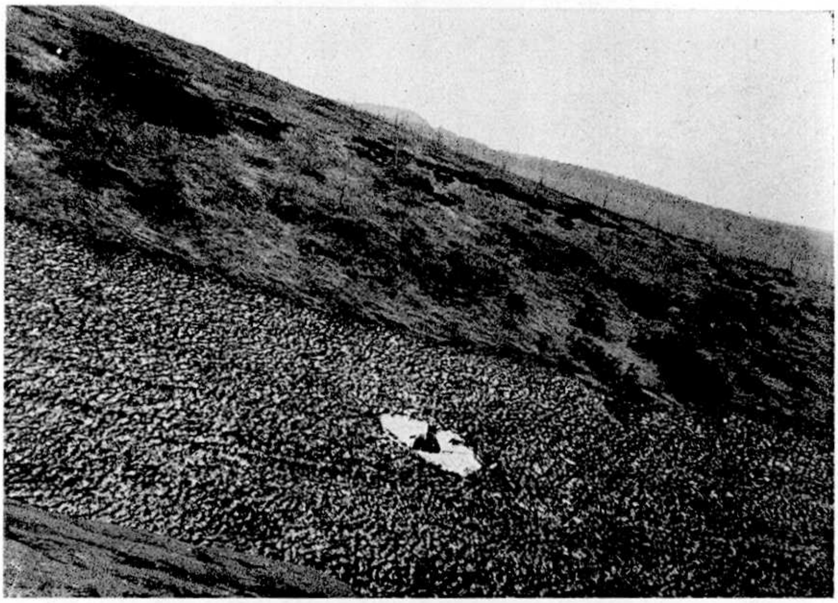

Fig. 30. A hole made on the snow by the fall of a bomb in the explosion of April 16, 1937.

(震研彙報 第二十號 圖版 水上)